ADVANCED MATERIALS
www.advmat.de

Materials Views
www.MaterialsViews.com

Degradation Mechanisms in Small-Molecule and Polymer Organic Light-Emitting Diodes

By *Franky So** and *Denis Kondakov*

Degradation in organic light-emitting diodes (OLEDs) is a complex problem. Depending upon the materials and the device architectures used, the degradation mechanism can be very different. In this Progress Report, using examples in both small molecule and polymer OLEDs, the different degradation mechanisms in two types of devices are examined. Some of the extrinsic and intrinsic degradation mechanisms in OLEDs are reviewed, and recent work on degradation studies of both small-molecule and polymer OLEDs is presented. For small-molecule OLEDs, the operational degradation of exemplary fluorescent devices is dominated by chemical transformations in the vicinity of the recombination zone. The accumulation of degradation products results in coupled phenomena of luminance-efficiency loss and operating-voltage rise. For polymer OLEDs, it is shown how the charge-transport and injection properties affect the device lifetime. Further, it is shown how the charge balance is controlled by interlayers at the anode contact, and their effects on the device lifetime are discussed.

1. Introduction

Organic light-emitting diodes (OLEDs) are promising for displays as well as for solid-state lighting. However, up to the 1970s, they were purely a scientific curiosity among scientists in the chemistry community. The early work on electroluminescence devices based upon anthracene single crystals[1] required very high operating voltages and the devices, of course, did not last very long. After the first publication on small-molecule OLED (SMOLED)heterojunction devices in 1987 by Tang and Van Slyke,[2] interest in the field began to grow. Initially, apart from the Eastman Kodak Company, interest in the field remained primarily with a small number of Japanese research groups.[3,4] It was only after the first demonstration of polymer light-emitting diodes in 1990 by Burroughes et al.[5] that the OLED field received world-wide attention.[6–14] In the early days, there was a lot of skepticism whether OLEDs can really progress into commercial products, because organic materials are known to be unstable under ambient conditions. The criticisms of the technology focused mainly on the fact that OLEDs require low-work-function electrodes as the cathode. Many early skeptics did not believe that the OLED fabrication process could be manufacturable, because the entire process requires stringent environmental control to avoid exposure of the cathode to oxygen and moisture. Exposure of devices to ambient conditions would lead to cathode degradation and generation of non-emissive areas—commonly known as dark spots in the OLED community today.

Throughout the 1990s, numerous publications[7,15–18] were devoted to the study of dark-spot growth and its growth mechanism. In general, dark spots occur if the devices are not sufficiently protected from the environment, and their growth would accelerate when the devices are under electrical stress. Dark sports in general originate from areas with pre-existing particle defects on the substrate. Subsequent deposition of the cathode layer leads to pin-hole formation in the metal thin film at the defect sites and results in diffusion of moisture through the pin holes, leading to localized delamination of the cathode and formation of non-emissive areas. These non-emissive areas often lead to the formation of bubbles or domelike[19] structures at the cathode interface. It has been reported that gas evolved because of the electrochemical processes at the cathode/organic interface causes the formation of these bubbles. Under continuous operation the delamination of the cathode at the defect sites would continue to grow and results in nonuniform emission from the devices. It should be noted that the dark-spot growth is mainly related to the degradation of the cathode, not the underlying organic layers. In fact, one can peel off the cathode layer from a degraded device and redeposit a fresh cathode layer on the same organic surface, and the resulting device would still function. Since the late 1990s, many researchers learned how to encapsulate the devices; growth of dark spots can be easily controlled if the devices are properly protected. It is interesting that initially many were skeptical about OLED technology because of the reactive cathodes used. Now, encapsulation has become a common practice in the field of OLEDs and dark spots no longer appear to be an issue. With improved encapsulations, corrosion of reactive metals no longer affects the lifetime of OLEDs, which is contrary to the initial concern.

During the early development, dark-spot growth was an obvious problem, and much attention was paid to the

[*] Prof. F. So
Department of Materials Science and Engineering
University of Florida
Gainesville, Florida 32611-6400 (USA)
E-mail: fso@mse.ufl.edu
Dr. D. Y. Kondakov
Eastman Kodak Company
Rochester, New York, 14650-2103 (USA)
E-mail: denis.kondakov@kodak.com

DOI: 10.1002/adma.200902624

development of encapsulation. Once the encapsulation problem is solved, the more challenging problem is to identify what the intrinsic degradation mechanisms are. To understand the origin of luminance degradation, one needs to examine the luminescence process and determine the physical processes at work. In an OLED, because of the very low carrier concentration present in the organic materials, charge carriers are primarily injected from the injection contacts. The carrier profile is determined by the nature of the injection contact and the bulk transport properties of the organic material. Efficient injection contact would lead to a high carrier density at the region nearest the contact. For the trap-free limit regime with Ohmic injection, the carrier profile[20] varies with $x^{-1/2}$, where x is the distance from the injection contact. The shape of the carrier profile is determined by the carrier mobility as well as the trap density. In the case of simple polymer devices, where the polymer layer is sandwiched between two injection contacts, space–charge limited transport has been observed[21,22] in dual-carrier devices, provided that the carrier injection is Ohmic. However, in the case of small-molecule heterostructure devices, the charge transport is far more complex and often limited by charge injection. Nevertheless, the photon flux from an OLED can be written as:

$$\Phi(t) = \int R_{\mathrm{rad}}(x,t)n(x,t)\,p(x,t)dx \quad (1)$$

Here, $n(x,t)$ is the time-dependence electron density profile, $p(x,t)$ is the time-dependent hole profile, and $R_{\mathrm{rad}}(x,t)$ is the exciton radiative recombination rate, which is also a function of position and time. Integrating the three parameters over the entire thickness of the emissive layer yields the time-dependent photon flux. Equation 1 actually means that if there is a change in luminance with time, there must be changes associated with the radiative recombination rate and electron or hole profiles. Let us consider these three quantities one by one. The radiative recombination of the emissive layer is a quantity related to the bulk properties of the materials. Any changes in the bulk properties caused by crystallization, morphological changes, or chemical reactions in the emissive layer can affect the bulk recombination rate. One way to determine its value is to measure the photoluminescence quantum yield. $n(x,t)$ and $p(x,t)$ are the carrier profiles, which are determined by both charge injection properties and the bulk transport. Any changes in the injection contact will affect the carrier injection efficiency and hence the carrier profile. There are many factors that could affect the injection properties. For example, changes in work function of the injection electrode can affect the injection properties. If the surface properties of ITO change with time, it could lead to changes in work function and hence affect its injection properties. In the case of polymer OLEDs, poly(3,4-ethylenedioxythiophene): poly(styrene sulfonic acid) (PEDOT:PSS)[23,24] is often used as an injection electrode, and changes in its work function during operating could also affect its injection properties. In fact, we will discuss this specific issue in the section on polymer-OLED degradation. Another factor that could change the injection properties is the formation of interface traps.[25] Interfacial trapped charges affect the electric-field distribution and hence the injection properties. In this Progress Report, we first discuss the various proposed intrinsic degradation mechanisms. We then present the degradation mechanisms of polyfluorene polymer and small-molecule heterostructure OLEDs to illustrate the different degradation mechanisms involved. OLED degradation is a complex issue. Depending upon the materials system and device architecture, the degradation mechanisms can be very different. Here, we use two different systems to illustrate the difference in the degradation mechanism. Our intent is not to present a unified theory on device degradation. We rather use these examples to present the complexity of the subject and, hopefully, shed light onto the device-degradation mechanisms in other organic optoelectronic devices.

Intrinsic Degradation: As discussed above, intrinsic degradation refers to the progressive and spatially uniform loss of luminance efficiency over time that occurs during operation. From a historical perspective, mechanistic studies initially focused on (i) thermal stability, (ii) trap and luminescence quencher formation, (iii) interface degradation, and (iv) anode instability. It is noteworthy that there is considerable conceptual overlap between, for example, trap formation and interface degradation, or interface degradation and anode instability.

Thermal Stability: In the early days, many believed that the OLED device operational stability was related to the thermal

Franky So is an Associate Professor in the Department of Materials Science and Engineering at the University of Florida. He received Ph.D. in electrical engineering from the University of Southern California. From 1993 to 2001 he worked at Motorola Phoenix Corporate Laboratories. From 2001 to 2005 he was the Head of Research at OSRAM Opto Semiconductors. His research interest is in the area of organic electronic devices and device physics.

Denis Kondakov received Ph.D. degree in 1991 from St. Petersburg University, Russia, in the area of physical organic chemistry of organometallics. After postdoctoral research studies on organic synthesis mediated by early transition metals with T. Takahashi at IMS, Japan, and E. Negishi at Purdue University, USA, he joined Eastman Kodak to investigate reaction mechanisms and photochemistry of photographic dyes. Since 2001, his work focused on device physics, photochemistry, and material design of small-molecule OLEDs.

stability of the organic materials. Several studies were devoted to the fabrication of high-glass-transition-temperature (high-T_g) polymers[26–29] or small-molecule materials.[30–32] Specifically in small-molecule devices, the initial short lifetime was attributed to the thermal stability of the hole-transport materials (HTMs). 4,4'-bis[*N*-(*p*-tolyl)-*N*-phenyl-amino]biphenyl (TPD) was used as the HTM in early SMOLEDs, and TPD was known to have a low T_g (≈60 °C). However, although TPD films deposited on glass readily crystallize at room temperature, crystallization is suppressed when the TPD films are overcoated with another organic thin film such as tris-(8-hydroxyquinoline) aluminum (Alq). In fact, careful examination of the full degradation reveals no sign of crystallization. To determine the correlation between thermal stability of the HTMs used in OLEDs and their device operational stability, Adachi et al.[33] tested more than ten HTMs with different T_gs and found that there is no correlation between thermal and device-operation stability. Low-T_g HTMs can exhibit a long lifetime, while high-T_g HTMs can exhibit a short lifetime. It should be pointed out that for high-temperature operation, a high-T_g is still needed, but for devices with good operation stability at room temperature, very high T_g is not required.

Trap Formation: During operation, the luminance degradation is mostly associated with the rise in operating voltage. In fact, in many cases of polymer light-emitting diodes (PLEDs), the luminance decay is almost a mirror reflection of the voltage rise, and there is a strong correlation between the luminance decay and the voltage rise during operation. Bulk degradation in the emissive layer is an obvious culprit for device degradation. If bulk degradation of the emissive layer is responsible for device degradation, it is likely that bulk traps are formed during operation. Formation of traps has two effects on device operation. First, traps lead to nonradiative recombination centers, which also lead to a decrease in luminescence. Second, bulk traps lead to decreases in the effective carrier mobility and hence increases in the operating voltage. In poly(phenylene vinylene) (PPV) devices, bulk degradation appears to be the main mechanism for device degradation. Parker et al.[19] studied the degradation of PPV light-emitting devices and found that the operating-voltage scale increased linearly with the thickness of the PPV layer. Based upon these data, they concluded that formation of traps is responsible for device degradation. The question is how the carrier transport is affected due to trap formation. Parker et al. further studied the voltage change in single-carrier devices during operation. These single-carrier devices are either electron-only or hole-only devices that allow transport of a single carrier type during operation. The authors found that the operation voltage of the hole-only devices remained unchanged with time, while a voltage rise in electron-only devices was observed with time. The magnitude of voltage rise in the electron-only devices is similar to that of the dual-carrier light-emitting devices. The data indicated that the electron mobility is substantially degraded due to electron transport, suggesting that the degradation in dual-carrier devices is related to trap formation, leading to a decrease in electron mobility. Silvestre et al.[34] conducted a similar study on PPV devices and they also came to the same conclusion. Interestingly, in contrast with polymer devices, the operation-related trap formation in small molecule OLEDs was demonstrated relatively late.[25] Instead, luminescence quenchers were believed to play a principal role in degradation processes.[35]

Interface Degradation: Most PLEDs have only two interfaces, one interface for electron injection and another one for hole injection. However, in SMOLEDs many interfaces are present in the devices, depending upon the device architecture, and the degradation is a more complex problem. In fluorescent OLEDs, the interfaces most susceptible to degradation are probably the hole-transport layer (HTL) and the emissive-layer (EML) interface because of the large energy difference of highest occupied molecular orbital (HOMO) of the two materials. For the conventional Alq devices, where amine compounds are typically used as the HTM, the difference in HOMO energy is typically 0.4–0.5 eV, which is a significant barrier for hole injection. In 1996, Hamada et al.[36] conducted an interesting experiment. In contrast to most fluorescent OLEDs, where the electron transport layer is the emissive layer, they fabricated devices where light emission originates from the HTL. That was accomplished by doping the emissive dopant (in this case rubrene) in the HTL instead of the ETL. They found that, while the conventional device (ETL is the emissive layer) has a very short lifetime (less than 50 h), the devices with HTL as the EML have lifetimes almost 100 times greater than those of conventional devices. The only difference between the two devices is the location of the emission zone. In the unconventional devices, holes do not need to be injected from the HTL to the ETL. Based upon these data is suggested that the HTL|ETL interface is the culprit of degradation. If that is indeed the case, enhancement in lifetime is expected if we can dispense with that interface. In 1997, Motorola proposed[37] the fabrication of devices by mixing both the HTM and ETM as the emissive layer.[38–40] The lifetime of the devices fabricated with this mixed host architecture is more than 10 times the lifetime of the devices with a heterostructure scheme. At about the same time, the Xerox[41] also reported enhanced lifetime with the mixed host architecture. Similar results[42–44] have also been reported by other research groups. Further enhancement in device performance can be achieved with an emissive layer with a graded composition, i.e., the region close to the hole injection electrode is HTM rich and the region close to the electron injection electrode is ETM rich. Mixed-layer architecture was also adapted to the phosphorescent devices and enhancement in device performance was demonstrated.[40–45] It is noteworthy that, despite numerous reports of improved stability of mixed layer devices, the studies of Eastman Kodak suggest that the mixed or graded layer approach is not universally useful, particularly for bilayer devices with very good lifetimes. In contrast with the mixed-host work reported by Motorola and Xerox[40,41] Eastman Kodak found that both mixed and graded NPB|Alq devices showed only minor stability improvements in comparison with a standard bilayer structure. The large differences in stability effects of mixing observed in different laboratories are not fully understood. However, the fact that there is also more than one order of magnitude difference in stability of standard bilayer NPB|Alq devices suggests a possible explanation that the NPB|Alq mixing is effective in improving stability of only the short-lived NPB|Alq devices, for example, by suppressing contamination-initiated degradation processes.

Anode Degradation: In the 1990s, many researchers discovered that indium is released from the indium tin oxide (ITO)

anode into the organic layers. Lee et al.[44] first suggested that indium out-diffusion is responsible for OLED luminance degradation. Using secondary ion mass spectrometry (SIMS), Lee et al. found that indium is present in the organic layers of the devices that have been stressed. They found that the indium content present in the organic layers of the stressed devices is significantly higher than that of the pristine devices. To demonstrate the effect of indium degradation, they further fabricated devices by doping 0.25% indium in the emitting zone of the device and found that the luminescence is strongly quenched because of the presence of indium. Based upon these data, they proposed that indium out-diffusion is responsible for luminance degradation. It should be noted, however, that 0.25% indium is an extremely high concentration, which is not realistic in actual devices. If indium out-diffusion is a key degradation mechanism, all devices should have short lifetimes because out-diffusion of indium appears to be present in many OLED devices. The fact that some devices have long operating lifetimes indicates that out-diffusion of indium does not appear to be a major mechanism to device degradation. Furthermore, the degradation process is evidently caused by device operation. Contrary to what can be expected from the out-diffusion of indium as a principal degradation process, device storage does not result in luminance efficiency loss. Although it can be argued that the migration of indium ions is driven by electric field and, therefore, only occurs during operation, the device lifetime is not significantly improved under alternating-current (AC)operation.

Instead of indium out-diffusion, oxygen out-diffusion in ITO might be more problematic. During the fabrication process, ITO has to be treated with either UV-ozone or oxygen plasma. A purely argon-plasma-treated ITO surface does not contain sufficient oxygen to provide the high work function needed for efficient hole injection. However, oxygen-plasma- or UV-ozone-treated ITO surfaces are not stable. These surface treatments in general force the oxygen atoms to the ITO surfaces and these oxygen atoms are not stable on the ITO surfaces. ITO surfaces can lose oxygen, resulting in a reduction in the work function. It should be noted that ITO was used as an injection electrode in the early PLED devices. Contrary to Lee's findings on indium out-diffusion, de Jong et al. found that out-diffusion of oxygen might affect the lifetime in many PLED devices.[46] By inserting a conducting polymer such as PEDOT:PSS between the ITO electrode and the polymer layer, a dramatic enhancement in efficiency and lifetime was reported.[19,23,24,46] The enhancement in efficiency is due to the fact that PEDOT:PSS has a higher work function (≈5.0 eV) than ITO, resulting in more efficient hole injection. The substantial enhancement of lifetime is probably due to the fact that ITO is no longer an injection electrode in these devices with PEDOT:PSS as the hole-injection layer. Here, ITO purely acts as a transparent conductor, not as an injection electrode, and the hole-injection properties depend only upon PEDOT:PSS. As a result, the device lifetime is no longer a function of the ITO stability. In fact, although PEDOT:PSS is highly acidic and can etch the ITO electrode, there are PLEDs using PEDOT:PSS as the hole-injection layer with very long lifetime and the reaction does not seem to be an issue. One should note that moisture does damage PEDOT:PSS, resulting in dedoping, lowering of its work function, and degradation of its hole-injection properties.[19,47] When properly baked and encapsulated, the PLED lifetime is always enhanced with the use of a conducting polymer such as PEDOT:PSS. This point will be further elaborated in a later section. Using conducting polymers as an injection contact does not only enhance the PLED lifetime, we have recently reported substantial lifetime enhancement in OLEDs when a conducting polymer is inserted between ITO and the HTL of the device.

2. Small-Molecule OLED Degradation

2.1. Generality of the Connection Between Luminance and Voltage Changes

Typically, modern efficient OLEDs based upon small-molecule materials use transport materials with high mobilities and low barriers to inject charge carriers from the respective electrodes. As a result, practically useful luminance levels (100–1000 cd m^{-2}) are frequently achieved at operating voltages that are close to bandgaps of emissive layers, e.g., ≈3 V for anthracene derivatives—common hosts in blue, green, and white devices. On the other hand, the built-in voltages are determined by the substantially smaller differences in work functions of the electrodes (or virtual electrodes formed by n- or p-doped organic semiconductors). For typical injection and electrode materials, the built-in voltages are ≈2 V as determined from open-circuit photovoltage data, which is nearly 1 V less than the bandgaps of emissive-layer hosts. Regardless of the sequence of the materials and heights of the respective barriers, this mismatch implies that the devices are injection limited.

With respect to device degradation processes, the injection-limited regime implies that any operation-related change in carrier injection will alter the electric-field profile and, consequently, distribution of charge carriers in a vicinity of a recombination zone. For example, deterioration of the anode|HTL interface will raise the electric field in the HTL and increase the electron-current leaking to the anode. It is noteworthy that, although the electron leakage to the anode is a clear source of efficiency loss, its contribution appears to be negligibly small in most of the efficient OLEDs as a result of the large barrier for the injecting electrons into common HTMs. In one study it was demonstrated that moderately impeding hole injection in classical NPB|Alq devices may result in higher efficiency because of a higher electric-field-reduced concentration of luminescence quenchers—NPB cation-radicals.[48] The deleterious effect of increased leakage of electrons was negligible relative to the efficiency-enhancing decrease in quenching. However, even if a minor deterioration of the anode|HTL interface may result in an increased efficiency, it is obvious that further decline in the hole-injection facility must eventually cause the leaking electron current to dominate, thereby decreasing efficiency and ultimately converting the device to an electron-only, nonemissive state.

In a symmetric fashion, qualitatively similar effects may be expected from the leakage of hole current for deteriorating electron injecting. However, using NPB|Alq devices again as an example, it has been shown that the deterioration of the electron

injection interface may result in a decrease in efficiency even when the leakage of hole current is insignificant.[49] Impeding electron injection is essentially equivalent to increasing electric field across an injecting interface in order to maintain fixed electron current. Because the device is injection limited and the space–charge relation is negligible, the electric field across the Alq layer in NPB|Alq device is equally increased. As dictated by the Poisson equation, which relates charge density and the change in electric-field strength, the positive charge density—concentration of quenchers—is consequently increased as well. Therefore, even minor deterioration of the electron-injecting interface may have a deleterious effect of device efficiency. It is noteworthy that the leakage currents—hole current reaching cathode and electron current reaching anode—are likely to remain insignificant when electric-field increase in ETL is minor. In other words, despite the loss of efficiency being associated with electron injection and respective voltage rise, the charge balance—fraction of the charge carriers recombining in the emission zone—is not significantly affected.

Interestingly, some asymmetry occurs in determining which effect impeding hole and electron injection have on the device efficiency: the former case shows initial boost followed by monotonic drop, whereas the latter case only shows monotonic drop. This asymmetry is of course not a fundamental feature of OLEDs; it stems from the differences in injection barriers for anode|HTL and ETL|cathode interfaces based upon typical OLED materials, such as NPB and Alq.

Because the characteristics of charge-injecting interfaces can affect device efficiencies by perturbing electric field over arbitrarily long distances, it is clear that operational degradation of OLED devices—loss of luminance efficiency and rise of operating voltage—might be caused by deterioration of such interfaces. The analysis of quantitative relationships between voltage rise and luminance efficiency loss can therefore provide important insights into mechanisms of operational degradation of OLED devices. Nonetheless, it is important to recognize that, in general, it is incorrect to assume that there is necessarily a deterministic relationship between luminance efficiency loss and voltage rise phenomena. For example, NPB|Alq devices with Mg:Ag cathodes show no appreciable voltage rise when operated to half of the initial luminance efficiency with the AC driving technique.[25] In contrast, operation with direct current (DC) results in a substantial increase in operating voltage, which corresponds to ≈0.2 MV cm^{-1} increase in electric-field strength in the Alq layer at 20 mA cm^{-2}. However, the time to reach half of the initial luminance is approximately equal in both cases, which suggests that efficiency loss is mechanistically unrelated to voltage rise in those devices. Indeed, it has been demonstrated that the luminance-efficiency loss in NPB|Alq devices is associated with accumulation of deep traps—nonradiative recombination centers at the NPB|Alq interface.[2] Because of their location the traps have a strong effect on the luminance efficiency but do not significantly influence operating voltage.

Further indications of the differences in causes of efficiency loss and voltage rise in those devices are obtained by evaluating post-operation behavior of DC-driven devices. The voltage rise observed in that case is mostly reversible after applying reverse bias for several hundred hours, which is consistent with studies by Yahiro et al.[49] In contrast, the reverse bias has only little effect (≈10%) on luminance efficiency, which supports the notion of the different mechanisms of efficiency loss and voltage rise.

2.2. Physical Studies of Voltage Rise and Luminance Loss Phenomena

The above discussion exemplifies few different possibilities of the interaction between efficiency-loss and voltage-rise phenomena in SMOLED devices. It is clear that, at least in principle, the device physics allows anything ranging from deterministic relationship to complete independence of the two phenomena. It is also clear that the details of device architecture determine which form this relationship takes. Considering the diversity in OLED device architectures and materials found in the open literature, the choice of experimental subject is very important for a study to be relevant. For example, although NPB|Alq devices may still serve as a useful system to study some aspects of device physics, they are hardly representative of practically useful devices. With that in mind, we chose to focus on highly efficient blue-fluorescent devices for this study. The triplet–triplet annihilation allows these devices to substantially exceed a classical limit of 5% for the external quantum efficiency (EQE) of fluorescent OLEDs.[50] The distinctive combination of high efficiencies, low operating voltages, long lifetime, and deep-blue color that can be achieved with fluorescent devices of this type explains why they remain indispensable for the practical application in display and lighting applications.

In terms of device composition and architecture, these OLEDs typically use anthracene derivatives as emissive layer hosts and as transport materials with high charge-carrier mobilities and low injection barriers. The device A1 [ITO/CFx|95-nm NPB (*N*,*N*′-diphenyl-*N*,*N*′-bis(1-naphthyl)-1,1′-biphenyl-4,4′-diamine)|20-nm α,β-ADN (9-(*p*-biphenyl)-10-(2-naphthyl)anthracene)[51] + 3% TTSB (4-(di-*p*-tolylamino)-4′-[(di-p-tolylamino)styryl]biphenyl)|20-nm PADN (9,10-bis(2-naphthyl)-2-phenylanthracene)|15-nm BPhen (4,7-diphenyl-1,10-phenanthroline)|0.5-nm LiF|Al] provides a representative example that uses only the materials already disclosed in open literature. Although device A1 also employs architecture that is simplified relative to proprietary OLEDs, it showed excellent initial characteristics: 7.6% EQE, 3.8 V, 10.2 cd A^{-1}, CIE_x 0.142, and CIE_y 0.173 (CIE = Commission internationale de l'éclairage) at 20 mA m^{-2} current density. As shown in **Figure 1**, operating the device A1 at 40 mA cm^{-2} current density results in a moderate voltage rise, which is approximately 0.5 V at half-life (≈140 h). Because of the encapsulation applied to all devices discussed in this section, the negligible formation of dark spots virtually rules out active area decrease as a reason for voltage rise. Although there is some curvature, the voltage rise is mostly a linear function of time, which makes it clearly dissimilar from the luminance efficiency decay curve. By themselves, the dissimilar shapes are insufficient to conclude that voltage rise and efficiency loss are two independent phenomena in the case of device A1. One obvious possibility allowed by device physics is that the linear rise in electric field and, accordingly, interfacial charge density, translates to a strongly nonlinear quenching effect. In fact, all common models of solid-state

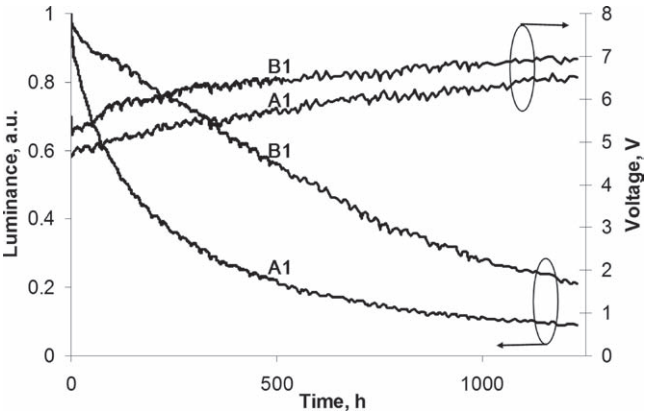

Figure 1. Luminance (left axis) and voltage (right axis) during operation at 40 mA cm^{-2} current density.

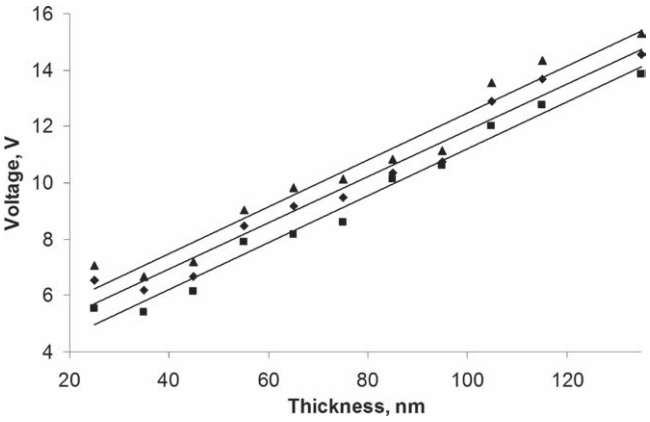

Figure 2. Operating voltage as a function of electron-transport-layer thickness before operation (squares), after 560 h (diamonds), and after 1230 h (triangles) of operation at 40 mA cm^{-2} current density.

photoluminescence do predict nonlinear dependences on quencher concentrations.

It is noteworthy that the moderate lifetime of device A1 can be substantially improved by various modifications of the transport and injection layers. For example, introducing the electron trapping dopant rubrene into the electron transport layer in the device B1 (ITO/CFx|95-nm NPB|20-nm α,β-ADN + 3% TTSB|25-nm PADN + 10% rubrene|10-nm BPhen|0.5-nm LiF|Al) results in slightly decreased initial performance characteristics relative to device A1: 5.1% EQE, CIE$_x$ 0.154, and CIE$_y$ 0.199 and 4.5 V operating voltage at 20 mA cm^{-2} current density. In contrast, the effect of doping the electron-transport layer on device stability is considerably more substantial: the half-life is improved by >4× relative to device A1. Although the exact mechanism responsible for relative differences in performance of devices A1 and B1 is outside of the scope of this discussion, it is plausible that the introduction of the trapping dopant away from anode|NPB and Bphen|cathode interfaces should not affect injection of the charge carriers. As illustrated in Figure 1, despite the large difference in luminance decay rates, the devices A1 and B1 show similar rates of voltage rise. These observations suggest that the electrode deterioration cannot be the main cause of operation-related luminance-efficiency loss in OLED devices represented by A1.

It should be stressed that the comparison of devices A1 and B1 is insufficient to make any conclusion about actual causes of voltage rise and efficiency loss. It is also insufficient to assess the likelihood of both phenomena being caused by the same mechanism. Interestingly, the possibility that the voltage rise is caused by the electrode deterioration can be readily tested in these device structures by evaluating the electric field in the corresponding transport layer. Although intralayer electric field strengths can be measured with Stark effect spectroscopy in some OLED devices,[52] it is often more practical to obtain electric fields from operating voltage evaluations in a series of devices with variations in a specific layer thickness. Within a layer with negligible space charge, the electric field is approximately constant and independent of layer thickness. The voltage drop across such a layer is simply a product of electric field strength and layer thickness, which allows evaluation of the electric field as a slope of linear dependences of the operating voltage on the layer thickness. We applied this technique to evaluate the electric field in electron transport and emissive layers of device B1 and a series of analogous devices with varied thickness of the PADN layer as a function of operation time. **Figure 2** shows that the operation-related voltage rise is reflected only in intercepts of the linear dependencies. In contrast, the slopes of linear dependencies of operating voltages on PADN layer thickness are virtually independent of operation time. This behavior is inconsistent with voltage rise being caused by cathode deterioration. Analogously, by varying the thickness of the NPB layer we found that the anode deterioration is not a main source of voltage rise in OLEDs similar to A1. Therefore, it is plausible that the voltage rise originates inside or in the immediate vicinity of the emissive layer.

Although various assumptions about distribution of charge carriers and electric fields within the emissive layers of OLEDs are fairly common in the literature, they are typically unsupported. The presence of the comparable concentrations of carriers of both signs within the narrow region makes finding useful analytical solutions impossible and numerical modeling extremely difficult. In addition, potentially applicable experimental methods typically do not have sufficient spatial resolution to analyze intralayer distributions of charges and electric field. In view of these difficulties, it is unlikely that physical experiments can shed additional light on the origin of voltage rise beyond finding that it originates inside or in the immediate vicinity of the emissive layer in OLEDs, such as A1. However, although the mechanism of voltage rise is of interest regardless of the connection with luminance efficiency loss, our focus is primarily on luminance-efficiency degradation. Therefore, rather than trying to find the exact cause of voltage rise, we need to address a more relevant question of whether deterioration of charge-injecting interfaces can be quantitatively consistent with *both* voltage-rise and luminance-efficiency-loss phenomena. This question can be answered effectively by employing devices modeling the degradation process. By comparing devices A1 and B1 it is easy to see that trapping dopant in the electron transport layer causes a significant increase in electric-field strength, as evidenced by a 0.7 V increase in operating voltage. This increase is attributed to trapping of electrons by rubrene

molecules in ETL, which creates negative space charge in the bulk of the PADN layer on the cathode side. Because the injection of electrons from the cathode is obviously unaffected by the introduction of rubrene at least 10 nm away, the electric field in the region between cathode and rubrene-doped ETL remains the same. Therefore, as dictated by the Poisson equation, the electric field on the other side of the space–charge region must increase, which necessarily leads to an increase in operating voltage exemplified by comparison of devices A1 and B1. Such doping can be used as an adjustable equivalence of cathode deterioration. However, the dopant in the PADN layer of device B1 is sufficiently close to the emissive layer to be involved in other processes, e.g., quenching the blue emissive dopant, participating in a tentative chemical reaction taking place during device operation, etc. Therefore, we modified the structure of device B1 to substantially increase the thickness of the PADN electron-transport layer in devices C1 and C2: ITO/CFx|95-nm NPB|20-nm α,β-ADN + 3% TTSB|115-nm PADN|20-nm PADN + x rubrene|10-nm BPhen|0.5-nm LiF|Al, where $x = 0$ and 10%, respectively.

The thickness of the PADN layer was chosen to approximately position the emissive layer at the second interference maximum, which is reflected in high efficiency (6.3% EQE) and deep-blue color (CIE_x 0.138, CIE_y 0.084) of device C1. Despite the large difference in PADN layer thickness, devices C1 and A1 showed similar half-lives, ≈140 h and ≈120 h, respectively. The introduction of the electron-trapping dopant rubrene in device C2 resulted in a substantial increase in the electric field, which was reflected in the initial value of the operating voltage: at 20 mA cm^{-2}, 4.8 V and 9.3 V for devices C1 and C2, respectively. Considering that the built-in voltage in devices C1 and C2 is ≈2.1 V and the voltage drop across the NPB layer is ≈0.4 V, the average electric fields across the emissive and electron-transport layers are estimated to be ≈0.15 MV cm^{-1} and ≈0.44 MV cm^{-1} in devices C1 and C2, respectively. Thus, despite the ≈3× increase in electric field strength, the luminance efficiency effect is minor: 4.9% EQE for device C2, which is only ≈1.3× lower than in device C1. Having established the relationship between the device efficiency and ability of the injecting interface to supply electrons, we can analyze the voltage-rise data in the active operation of device C1 as a possible source of luminance-efficiency loss.

Device C1 showed a voltage rise of ≈1 V at half-life, as was measured at 20 mA cm^{-2}. Even assuming that the voltage rise is exclusively due to the deterioration of the electron-injecting interface, the electric-field strength in the electron-transport and the emissive layers is increased at most by 1.4×, yet the luminance efficiency is lowered by 2×. Therefore, comparing relative differences in voltage and efficiency characteristics of the pair of fresh devices C1 and C2 against the pair of fresh and degraded devices C1, we conclude that the degradation of the electron-injecting interface is insufficient to explain luminance efficiency loss.

We tested the possibility that deterioration of the hole-injecting interface is the main reason for luminance-efficiency loss in a similar fashion by using a hole-impeding layer of NPB diluted with ADN in devices D1–D4: ITO/CFx|20-nm NPB|20-nm NPB + x 20-nm α,β-ADN|55-nm NPB|20-nm α,β-ADN + 3% TTSB|115-nm PADN|20-nm PADN + x rubrene|10-nm BPhen|0.5-nm LiF|Al, where $x = 0\%$, 60%, 80%, 85%, respectively. The initial operating voltages and efficiencies were 5.7 V/6.0%, 5.9 V/6.1%, 6.2 V/4.5%, and 8.3 V/3.1%, for devices D1–D4, respectively. In agreement with predictions from prior studies,[1] an increase in electric field from D1 to D2 causes a minor increase in device efficiency. Further increases in electric field in the NPB layer adjacent to the emissive layer led to a substantial lowering of luminance efficiency. It is noteworthy that the electric-field strength in the NPB increases considerably more than the operating voltage. In device D1, the electric-field strength in NPB is ≈0.042 MV cm^{-1}, which is estimated from slopes of linear dependences of between operating voltages and thicknesses of analogous devices with varied NPB thicknesses. Assuming that the higher-electric-field region is limited to 55 nm of NPB between the impeding and emissive layers, the electric-field increases relative to device D1 are 1.8×, 3.2×, and 12×, for devices D2–D4, respectively. Thus, an order-of-magnitude increase in electric-field strength in the HTL is required to half the luminance efficiency.

Considering that device D1 showed ≈0.8 V voltage rise at a half-life of ≈190 h, the degradation-related increase in electric-field strength in the HTL can be at the most 3×. Based upon model devices D2–D4, even this upper estimate of the degradation-related increase in electric field strength is insufficient to explain the 2× decrease in luminance efficiency at half-life.

Overall, the comparisons of the voltage and efficiency characteristics of the degraded devices and the respective model devices invariably lead to the conclusion that the deterioration of charge-injecting interfaces, e.g., interfaces between electrodes and charge-transport layers, does not plausibly explain operation-related luminance-efficiency loss. Furthermore, as demonstrated by the variation of transport-layer thickness in device B1, the voltage rise is also unlikely to cause the deterioration of charge-injecting interfaces. It is therefore likely that the deleterious processes in the immediate vicinity of the emissive layer are responsible for the operational degradation of OLEDs such as device A1.

2.3. Chemical Nature and Location of OLED Degradation

It was previously shown that various chemical processes occur in operating OLED devices.[53–56] Some of them involve materials present in an immediate vicinity of the emissive layers in most of the OLED devices. NPB is a representative material of this type. By analogy with the previous studies, it is plausible that the operation of device A1 also results in free-radical reactions involving NPB and α,β-ADN. Indeed, the chemical analysis of device A1 operated for 1230 h at 40 mA cm^{-2} showed a similar set of NPB-derived degradation products.

Based upon the observation of the identical set of chemical products in photoexcited NPB films and the comparative analysis of homolytic and heterolytic bond dissociation energies, the NPB transformations were proposed to be initiated by homolytic cleavage of the carbon–nitrogen bonds in the singlet excited state of NPB.[55] The unimolecular dissociation is the simplest mechanism that is consistent with the available experimental data. More complex mechanisms can be also envisioned, for example, to involve more than one NPB molecule or NPB molecules in a charged state. However, it is not clear if invoking

a more complex mechanism is conceptually beneficial. For example, based upon chemical intuition, it is reasonable to expect that the oxidation of stable, neutral, closed-shell organic molecules would result in bond weakening. This expectation is founded on the assumption that frontier orbital electrons participate in bonding to a significant degree. However, this argument is not generally correct. In the specific case of NPB, oxidation involves a nitrogen lone pair of electrons that does not participate in the formation of a carbon–nitrogen σ-bond. The density functional calculations predict that the dissociation of the weakest carbon–nitrogen bonds in NPB requires nearly equal (within 2 kcal mol^{-1}) energies in neutral and cation-radical states. On the other hand, the vertical energy of the lowest singlet excited state of the cation radical of NPB is much lower: 0.9 eV is predicted by the time-dependent density functional method and ≈1.0 eV is estimated from the experimental absorption spectrum. Thus, the homolytic dissociation of the excited state of the NPB cation radical is essentially forbidden by energy.

The cation radical of NPB has substantial absorption in the visible part of the spectra, which allows it to act as an efficient long-range quencher.[48] After the energy transfer, the excited cation radical undergoes rapid internal conversion to the lowest singlet excited state, which is likely to be significantly below the ≈1.0 eV energy estimated for a vertically excited NPB. Because of energy-gap-law requirements, the low energy of the relaxed excited state of NPB is also expected to result in fast deactivation by internal conversion to the ground state.[57] Although both low energy and fast deactivation of the excited state make it unlikely to initiate any observed chemical reactions associated with OLED device degradation, the opposite effect of stabilization due to the presence of an NPB cation radical is plausible.

Because of the uncertainties associated with measurements of the concentration profiles of active species in operating OLEDs, we tested the potential involvement of NPB cation radicals in excited-state reactions using the photoexcitation technique. The experiments were performed on 100-nm NPB films both in the presence and in the absence of current. The films were deposited on regular ITO/CFx substrates and capped with a layer of Al, which resulted in the formation of holes-only devices. The 72 h of irradiation with 436-nm light with 0.5 W cm^{-2} power density resulted in no detectable changes in photoluminescence efficiency regardless of the application of 20 mA cm^{-2} current density. Because the 436-nm light corresponds to one of the absorption maxima of the NPB cation-radical,[49] it is not significantly absorbed by neutral NPB, thus we conclude that this observation supports the predicted absence of chemistry involving NPB cation-radical in operating OLEDs.

Based upon their structures, the observed products of chemical reactions of NPB in OLEDs may not be expected to suppress the electroluminescence or increase the operating voltage. Their inability to quench electroluminescence is supported by **Figure 3**, which shows that these molecules have no absorption in the visible part of the spectrum (>400 nm) and, therefore, would not be able to accept energy from a typical fluorescent OLED emitter. The deleterious effects of the degradation products must be due to the precursors of the detected products, which are formed in a complex free-radical chain mechanism.[55] Although these precursors are too reactive to be isolated and identified, it is plausible that the stabilized π-radical species,

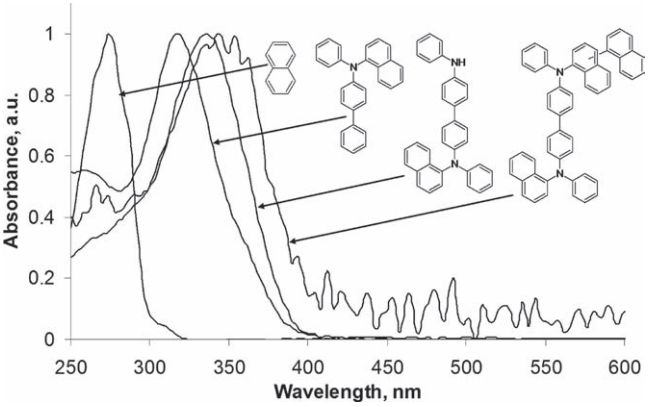

Figure 3. Normalized absorption spectra of the detected products obtained during chromatographic analysis of degraded devices.

such as shown in **Figure 4**, are formed and accumulated in the immediate vicinity of the interface between the hole-transport and the emissive layer in an operating OLED. The radicals shown in Figure 4 represent a small subset of possible products of radical addition reactions. Nonetheless, we expect these structures to be reasonably representative with regards to their effects on electroluminescence.

In the absence of suitable experimental methods to evaluate their properties, we used density functional quantum-chemical calculations to assess their propensities to act as deep traps—nonradiative recombination centers and luminescence quenchers. As shown in **Table 1**, regardless of the substitution position, both oxidation and reduction processes of these radicals are nearly 1 eV easier relative to the NPB. Even considering possible computational inaccuracies, it is clear that these molecules represent deep traps of charge carriers of both signs in the NPB matrix.

In order to assess the radiative properties of these molecules, we used time-dependent density functional calculations (see Table 1). The energies of the lowest spin-allowed transitions are ≈1 eV lower relative to NPB, which indicates that these molecules would quench matrix material. Low oscillator strengths of these transitions make them unlikely to emit light after excitation.

It is easy to see that the charge trapping and excited state quenching properties of the tentative degradation products are linked to the presence of a singly occupied molecular orbital.

Table 1. Properties of the tentative degradation products and NPB as a comparative material calculated by unrestricted B3LYP/6-31G* and TD-B3LYP/6-31G* methods.

Structure	Electron affinity [a] [eV]	Ionization potential [b] [eV]	Lowest allowed transition [eV]	Oscillator strength
Ia	1.02	4.87	2.25	0.13
Ib	0.95	5.68	2.00	0.004
Ic	0.79	4.69	1.95	0.04
NPB	0.19	5.60	3.07	0.25

[a] Calculated as energy difference between relaxed radical and relaxed anion forms without zero point energy corrections. [b] Calculated as energy difference between relaxed radical and relaxed cation forms without zero point energy corrections.

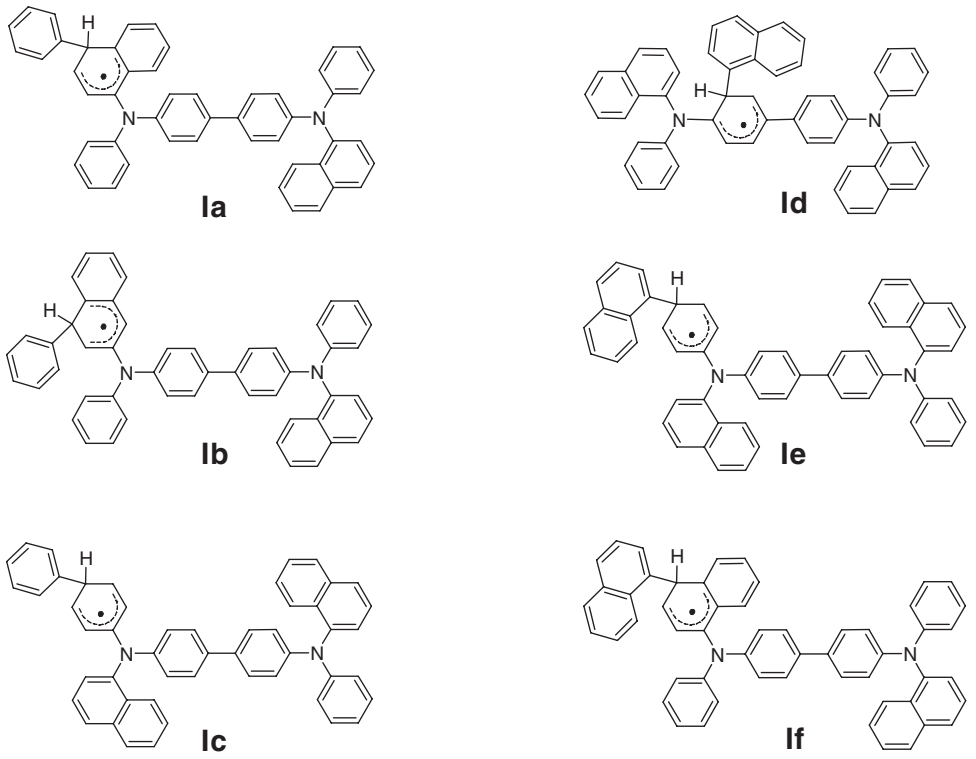

Figure 4. Structures of the free radicals—tentative degradation products of NPB.

Therefore, the deleterious properties of degradation products can be expected as a material-independent attribute. For example, we have previously seen that the anthracene derivative used as the emissive layer host undergoes chemical reactions in the region of immediate contact with the NPB HTL. Considering the high reactivity of radicals initially formed after NPB homolytic dissociation, it is plausible that anthracene would undergo free-radical attack, yielding a stabilized p-radical derived from the anthracene chromophore. Therefore, the operation-related accumulation of deep traps—nonradiative recombination centers and luminescence quenchers—is likely to be occurring not only in the HTL but in the emissive layer as well.

Interestingly, the ability of the tentative degradation products to trap charge carriers of both signs implies that, in some cases, the operation-related voltage rise might have the same origin as luminance-efficiency loss. Because of the differences in densities of mobile holes and electrons on the two sides of a recombination zone, we expect the positively charged traps to dominate on the anode side and negatively charged traps to dominate on the cathode side of the recombination zone. This behavior is illustrated by **Figure 5**, which schematically shows the distribution of filled traps and the electric-field profile in an idealized device before and after degradation. When current is flowing, the macroscopic dipole layer is formed by the preferential charging of hole traps on the anodes side of the degraded region and electron traps on the cathode side of the degraded region. Therefore, even when work functions of the electrodes and injection barriers remain unaffected by device degradation, the model exemplified by Figure 5 demonstrates that accumulation of traps may result in a voltage rise. Interestingly, unlike the electrode deterioration processes, the voltage rise that is due to a macroscopic dipole formed within the recombination zone is expected to be independent of transport layer thicknesses (compare with Figure 2). This is an important experimental criterion to allow making a distinction between degradation mechanisms related to electrode and recombination-zone deteriorations. It is noteworthy that the formation of similar macroscopic dipoles does not necessarily require accumulation of traps of the both signs. It is easy to see that a similar behavior would result if one of the sides of the internal macroscopic dipole would be due to mobile charge, blocked by the barrier such as classical HTL|ETL heterojunction.

Quantitatively, it is plausible that the voltage rise attributable to formation of internal macroscopic dipole is a monotonic function of trap concentration and, therefore, of the length of time the device is operated. Similarly, the luminance efficiency is determined by the concentration of the degradation products acting as nonradiative recombination centers and luminescence quenchers. From this perspective, it is not surprising that luminance efficiency loss and voltage rise are fundamentally linked phenomena even in the absence of a deterioration of electrodes and charge-injecting interfaces.

3. PLED Degradation

Polyphenylene vinylene (PPV)[5] was the first conjugated polymer used for PLEDs by Burroughes et al. in 1990. It was a single-layer device sandwiched between an ITO and an aluminum electrode. The devices had very low efficiency and poor lifetime.

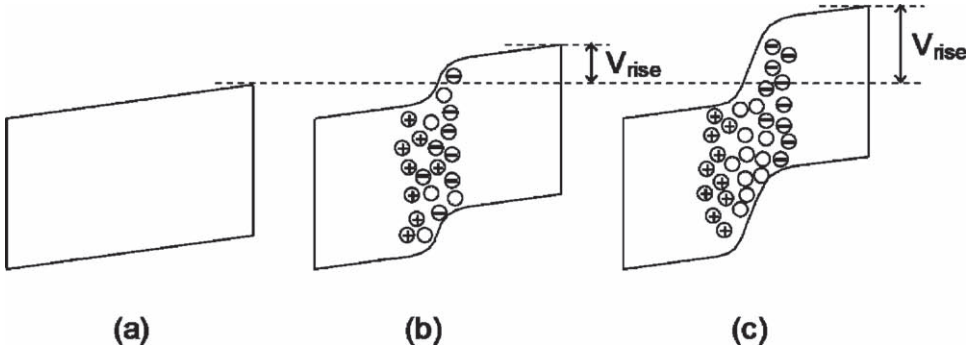

Figure 5. Schematic representations of the changes in electric fields and the trapped charge densities in the region of heterojunction of an OLED device operated at an equal current density before (a) and at two different stages of degradation (b,c). The anode (not shown) is assumed to be on the left-hand side. Empty circles represent unfilled traps—degradation products. Trapped holes and electrons are represented by circled '+' and '–' signs, respectively. For clarity, differences in HOMO and LUMO levels between the materials forming heterojunction are omitted. Also for clarity, identical overall barriers for injecting holes and electrons into the heterojunction region are assumed and depicted as equal slopes on the sides of the depicted region. The recombination zone is assumed to reside approximately in the middle of the depicted region. Absence of the deterioration of charge-injecting interfaces is reflected in unchanging slopes (electric fields) at the sides of the depicted region between devices (a–c). Although both increase in concentrations of the deleterious degradation products and widening of the degraded region are depicted as contributors to the increase in voltage (V_{rise}) in (b) and (c) relative to (a), we note that even one of these phenomena is sufficient to account for operation-related voltage rise.

Realizing the inefficient electron injection from the aluminum contact, low-work-function cathodes[10] were incorporated into the devices and the performance was somewhat improved. In 1996, Karg et al.[14] demonstrated enhanced luminance and lifetime using polyaniline as a hole-injection layer. Shortly afterwards, Carter et al. demonstrated a dramatic enhancement in lifetime with PEDOT:PSS[23] as a hole-injection layer. At the time, the function of the conducting polymer in PLEDs was not clear. Many called the conducting polymer used in the PLEDs "the buffer layer," suggesting that it does not play an active role in device operation. In fact, it was believed that it serves two purposes not related to device operation. First, the conducting polymer planarizes the ITO surfaces and reduces shorts, and the "buffer layer" was used to improve the device yield. Second, it serves as a barrier to oxygen reaction because it was believed that oxygen from ITO reacts with the vinyl carbon in PPV and is responsible for device degradation. Since then, using a conducting polymer as a hole-injection electrode has become a common practice. While PPV had a decent device lifetime with PEDOT:PSS as an HIL, its color availability is rather limited. PPV was available in orange and yellow colors because of the extent of the conjugation, and it became clear that a different conjugated polymer is needed for PLEDs. In the late 1990s, Dow Chemical developed a series of polyfluorene (PF) and copolymers[58] for OLED applications, and this class of polymer has become one of the most popular conjugated polymers for PLEDs in the last ten years.

One of the most widely studied classes of electroluminescent polyfluorene polymers is the family based upon poly(9,9-dioctylfluorene) (PFO or F8) and its derivatives, which can be designed to emit across the whole visible range of the spectrum.[27,59] Here, our lifetime study is based upon the LUMATION Green 1300 Series Light-Emitting Polymer (LEP), a polyfluorene-based alternating conjugated copolymer.[21,22] This polymer is used as an example for lifetime studies because of its high efficiency and good stability.

3.1. PEDOT:PSS and Other Hole-Injection Polymer Effects

In the early days of PLEDs, it was believed that the acidity of PEDOT:PSS might be the culprit of device degradation. PEDOT:PSS is highly acidic with a pH value less than 2. PEDOT:PSS is known to etch the underlying ITO layer when it is cast onto the ITO surface during the device-fabrication process. Using Rutherford backscattering spectrometry, de Jong et al.[46] found that in the as-prepared ITO|PEDOT:PSS|PPV devices there is 0.02 at% of indium present in the PEDOT:PSS film. Annealing in nitrogen increases the indium concentration to 0.2% and further exposure to air increases the amount of indium to 1.2%. It was believed that etching of ITO that is due to PEDOT is responsible for PLED degradation. One obvious technique is to neutralize PEDOT:PSS and reduce its pH value. De Kok et al.[60] have neutralized PEDOT:PSS using a solution of NaOH. The authors were able to tune the pH value from 1.4 to 7, by adjusting the concentration of NaOH. Increasing the pH value in PEDOT:PSS in general decreases its conductivity. For LUMATION Green PF devices, they found that for 1000 ppm Na^+ the hole current in single-carrier devices actually decreases by two orders of magnitude, suggesting the presence of a hole-injection barrier. The reduction of hole current leads to substantial lowering of the device efficiency. However, the effect of the PEDOT:PSS pH value upon device performance is substantial. The device efficiency decreases by almost 90% when the pH value of PEDOT:PSS increases from 1.5 to 7. It should be noted that the decrease in efficiency also associates with a decrease in lifetime due to charge imbalance and neutralizing PEDOT:PSS does not lead to better lifetimes. Therefore, acidity in PEDOT:PSS does not appear to be a culprit for the device lifetime problems.

Another problem associated with PEDOT:PSS is degradation due to the presence of moisture. Dark-spot formation is commonly observed in OLEDs where small particulates are present. It was always assumed that the formation of dark spots is due to corrosion of the cathode. While this might be true in

small-molecule OLEDs most of the time, dark spots in PLEDs are more complicated. Kim et al.,[61] have used micro-Raman spectroscopy to study the degradation of PLEDs composed of poly(2,7-di-n-octylfluorene-alt-benzothiadiazole) (F8-BT) due to moisture exposure. They found that the black spots are associated with cathode pinhole defects and the pinhole is surrounded by a non-emissive disk, in which the PEDOT is locally de-doped (or reduced) to a nonconducting state with concurrent local oxidation of the metal cathode. However, the electroluminescent (EL) polymer is largely unaffected. These results indicated that localized electrochemical activity is associated with the formation of black spots, not just oxidation of the metal cathode. The authors[61] proposed that water molecules dissociate into H^+ and OH^- ions when entering the pinhole defects, and the H radicals can diffuse to the PEDOT:PSS layer resulting in a reduction of the PEDOT:PSS layer. These results change the built-in potential resulting in reduction in hole injection.

In addition to PEDOT:PSS, other hole-injection polymers with larger work functions have been made to enhance hole injection.[19,62] Large work function hole injection polymers have resulted in reduced operating voltage as well as lifetime enhancement. Lee et al., formulated PEDOT:PSS with perfluorinated ionomer and they were able to increase the work function as large as 5.7 eV.[44] Using this approach, they were able to achievement significant improvement in PLED lifetime.

3.2. Charge Balance

The balance of carriers is not a common problem in inorganic semiconductor devices because both the carrier mobilities and the carrier concentrations are high. In organic semiconductor devices, however, the background carrier concentrations are low in general, and carriers responsible for the device operation are injected from the contact electrodes. Because of the space–charge effect that is due to the injected carriers, the carrier profile is not uniform. Because an exciton is formed by one electron and one hole, the balance of carriers in OLEDs becomes an important issue. While the balance of carriers in small-molecule heterostructure fluorescent OLEDs in general is not a serious problem due to carrier confinement by the carrier blocking layers, recently we reported that charge balance in phosphorescent OLEDs can strongly influence the device performance due to quenching of the triplet excitons by the carrier-blocking layers with low triplet energies.[44,63,64] On the other hand, charge balance in PLEDs is critical to device efficiency. As discussed above, PLEDs are single-layer devices without charge-blocking layers that control the charge flow. In PLED devices, the balance of carriers can only be controlled by the injection contacts and the carrier transport. The carrier-transport properties of a conjugated polymer are the intrinsic properties of the materials, and they are determined by the molecular structure, the extent of the conjugation, and the polymer morphology. The injection property, on the other hand, is determined by the relative alignment of the HOMO (or LUMO) level of the polymer. For electron injection, this is not an issue because most polymer LUMO levels match the work function of low function metals such as calcium, lithium, and cesium. However, hole injection could be problematic because the UV-ozone-treated ITO work function is less than 4.7 eV. While PEDOT:PSS has a slightly higher work function (5.0 eV),[47,65] its hole-injection efficiency might be a problem if a polymer has a deeper HOMO energy.

PPV was the early polymer used for PLEDs and it has a HOMO energy of about 5.0 eV.[65] Hole injection from PEDOT:PSS into PPV is fairly efficient. In terms of carrier transport, electrons are heavily trapped in PPV and the transport is hole dominant. The typical hole mobility of PPV-based polymers is in the order of 10^{-6} cm^2 $V^{-1}s^{-1}$. However, the electron mobility can be three to four orders of magnitude lower. As a result, the hole becomes the dominant carrier in the device and the recombination zone is close to the cathode interface. In fact, a slight decrease in hole injection or transport could lead to high efficiency because the recombination zone moves away from the cathode. That might be the reason the efficiency of some PPV devices increases slightly with time. Because of the prior history of PPV, many believed that conjugated polymers should be hole conducting. When PF-based devices were fabricated, the results were different from the PPV-based devices. **Figure 6** shows the current–voltage characteristics of single-carrier devices using the LUMATION 1300 PF as the lighting-emitting polymer.[37] Here, the electron-only device has the following structure: ITO|LEP (80 nm)|CaAl, and the hole-only device has the following structure: ITO|PEDOT:PSS (60 nm)|LEP (80 nm)|Au. Given that the HOMO level of the PF polymer is 5.8 eV,[37] the hole-injection barrier is larger than 1 eV and hole injection is negligible in the electron-only device. In the case of a hole-only device without PEDOT:PSS, Au was used as the top electrode and, because of the large work function in Au, its electron injection into the polymer is negligible. In both electron- and hole-only devices, light emission was not detected, indicating that these are good single-carrier devices. Contrary to what was found in PPV devices, the electron current in the electron-only device is almost two orders of magnitude higher than the hole current in the hole-only device. These data suggest two possibilities: either the electron mobility is higher than the hole mobility or the electron injection efficiency is higher

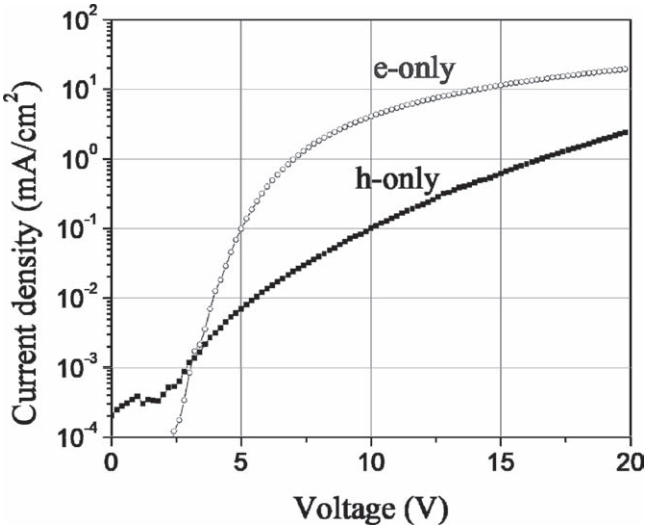

Figure 6. Current density versus voltage for electron-only (e-only) and hole-only (h-only) devices.

than the hole injection efficiency. In order to understand the carrier transport and injection properties of the polymer, dark-injection measurements were carried out.

Carrier Transport: Time-of-flight experiments are probably the most popular method to measure carrier transport. However, the techique requires very thick samples, typically thicker than 1 μm, because the thickness must be significantly larger than the sample skin depth. For polymer films, the polymer morphology might be very different for different film thicknesses and it is desirable to have a technique that does not require thick samples. Dark injection is another technique for carrier-transport measurements. The advantage of this technique is two-fold. First, less than 1-μm-thick samples can be used for the measurements. Second, the injection properties can also be obtained by the dark-injection technique. To carry out these measurements, both electron- and hole-only devices were fabricated. Here, a sample thickness of 0.28 μm was measured. The measurement was accomplished by applying a step voltage to the sample. The samples should be biased in such a way that carriers are injected from the ohmic injection contact. In hole-only devices, holes are injected from the PEDOT:PSS contact, and in electron-only devices, electrons are injected from the Ca/Al. It should be noted that although there might still be hole injection from the ITO contact into the LEP, it can be neglected because light emission was not observed, indicating that hole injection is insignificant. The position of the injection current maximum (dark-injection time, t_{DI}) is related to the transit time of injected charges, and thus the charge mobility μ can be calculated from the values of t_{DI} for the range of applied electric fields. The electron and hole mobilities by dark-injection techniques[21] are shown in **Figure 7** where the hole mobility μ_h is plotted as a function of $E^{1/2}$, where E is the electric field across the device. From the figure it is apparent that the electric-field dependence of both electron and hole mobilities follows the Poole–Frenkel-like behavior, i.e., $\ln \mu \propto E^{1/2}$, ubiquitously observed in most organic small molecules and conjugated polymers. It is clear that electrons are the dominant carriers (they have a higher mobility), especially in the low electric field region. The difference in mobility is somewhat lowered at high electric fields because of a steeper electric-field dependence of the hole mobility. The results in Figure 7a present one of the few examples where the electron mobility in a conjugated electroluminescent polymer exceeds the hole mobilities. As discussed previously, in most conjugated polymer systems, such as, e.g., polyfluorenes, poly(*p*-phenylene vinylene), and derivatives, holes are believed to be the dominant type of the carrier. It should be noted that the electron mobility can only be measured when the samples are encapsulated or stored in an inert environment. Samples exposed to air exhibit extremely dispersive electron transport where the transit time cannot be defined at all.

Carrier Injection: For a device with an ideal Ohmic contact, the steady-state dark-injection current should be equal to the space–charge-limited current, J_{SCL}. If the contact is non-Ohmic, then a measure of the contact injection efficiency can be obtained by comparing the theoretical J_{SCL} and the experimental dark-injection current.[21]Figure 7b shows the variation of the injection efficiency η as a function of electric field in the hole- and electron-only devices. In the electron-only device, the

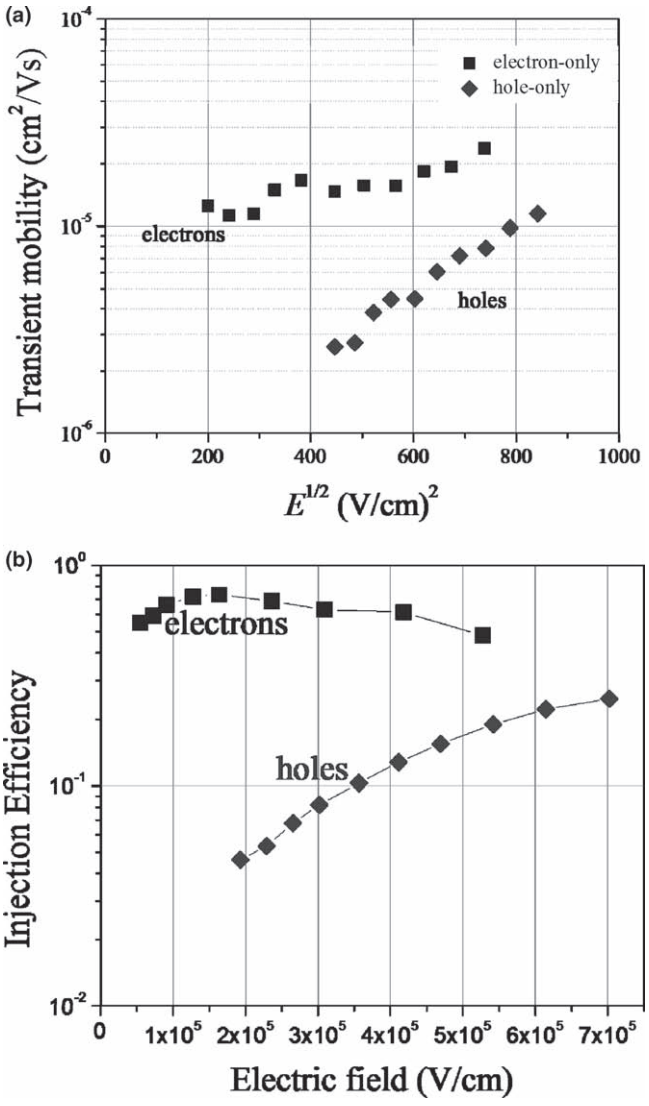

Figure 7. a) Transient electron and hole mobilities as a function of electric field for the LUMATION 1300 green polymer. b) Electron- and hole-injection efficiencies. Figure reproduced with permission.[22] Copyright 2005, American Institute of Physics.

value of the electron-injection efficiency varies between 0.5 and 0.7 (close to unity) and we can postulate that electron injection is close to Ohmic. Hole injection, however, exhibits a markedly different behavior: the hole-injection efficiency is less than 0.05 at an electric field 2×10^5 V cm^{-1} and increases up to 0.25 at $E \approx 7 \times 10^5$ V cm^{-1}. Such a low injection efficiency and its electric-field dependence indicates that hole injection from PEDOT:PSS is non-Ohmic. The non-Ohmic injection might be due to the difference between the HOMO energy of the LEP and the work function of PEDOT:PSS. It could also be due to the PEDOT:PSS polymer morphology and the chain orientation.

Because of the low hole mobility and low injection efficiency, it is expected that the resulting PLED is electron dominant and the transport is imbalanced. There are two consequences. First, that means some of the electrons are leaving the LEP without ever combining with the injected holes, leading to lower efficiency.

Second, electrons injected into the PEDOT:PSS layer might cause damages to the conducting polymer.[37] PEDOT is a conjugated polymer that can be oxidized (or doped) to a high-conductivity state.[23] In PEDOT:PSS, PEDOT is doped by PSS to enhance its conductivity. However, upon bombardment with even lower energy (as low as 3 eV) electrons,[37] it has been found that the PEDOT surface undergoes bond breaking and composition changes. Specifically, low-energy electron bombardment leads to the release of oxygen and sulfur, resulting in changes in conductivity and work function. It should be noted that, under some operational conditions (e.g., when the PLED is pulsed during multiplexing conditions), it is entirely possible that 3 eV electrons are leaving from the LEP layer. Given the fact that hole injection is a weak point of the device operation, it is not surprising to see that hole injection can further be weakened because of the "high-energy electrons." The weakened hole injection leads to further deterioration of charge balance and reduction of device efficiency.

Figure 8a and b shows the luminance and the PLED efficiency as a function of drive voltage for a pristine and an aged device. For the pristine device, the turn-on voltage is at about 2 V and its efficiency reaches the maximum efficiency at a voltage of 4.5 V. These data indicate that the device is not charge balanced at its turn-on voltage and the optimum charge balance is not reached until the operating voltage is 2.5 V above its turn-on voltage. This behavior is different from the PPV-based PLEDs in that the efficiency reaches its maximum value at low voltage.[66] The charge balance became worse in the aged devices. In the aged device, its maximum efficiency is not reached until the voltage reaches almost 6 V. The increase in operating voltage is also consistent with the findings by Giebeler et al.,[67] in that the degradation leads to changes in the built-in voltage, as measured by electroabsorption. The degradation of charge balance is probably due to the degradation of PEDOT:PSS and hence hole injection. Using dark-injection techniques, Khan et al.[68] measured the hole mobility and injection of PLEDs for stressed and unstressed LUMATION 1300 PLEDs devices. Based upon their study, they determined that there is a substantial degradation of the hole injection in the aged devices. They also found that, while the change in the hole mobility caused by electrical stress is negligible, the reduction of hole-injection efficiency is almost 90%. Khan et al.[68] also used electroabsorption to measure the change in the diode built-in voltage and found that there is a 0.8 eV decrease in built-in voltage. These results suggest that electrons injected into PEDOT:PSS cause de-doping and shift its Fermi level away from the valance-band edge, resulting in an increase in hole barrier and a reduction in hole-injection efficiency. They proposed that the degradation is due to formation of a resistive interfacial layer between the PEDOT layer and LEP. These results are in agreement with our findings related to degradation in charge balance.

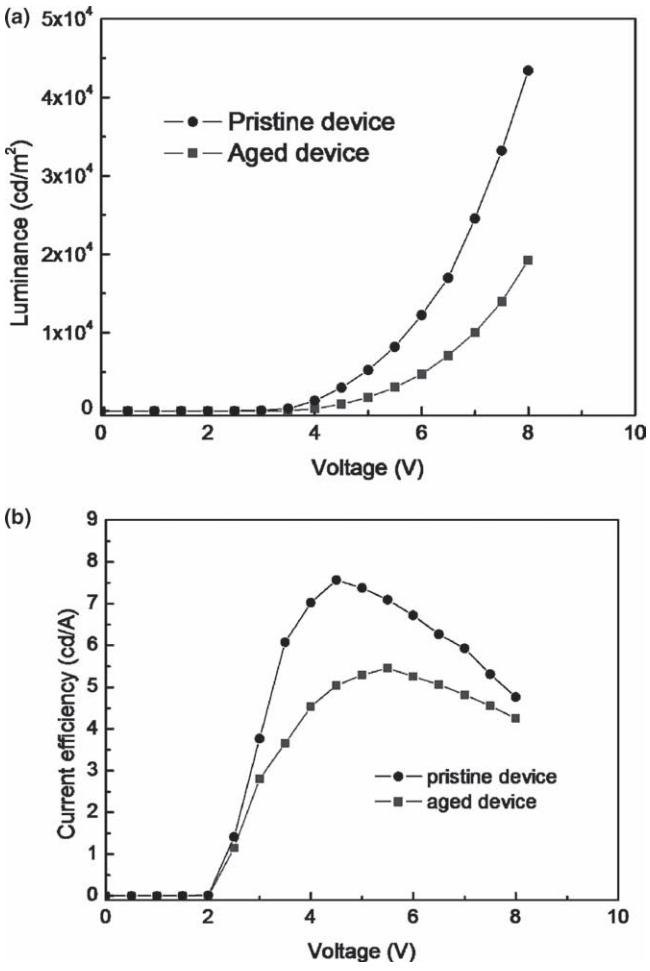

Figure 8. a) Luminance–voltage characteristics for the pristine and aged devices. b) Current efficiencies as a function of voltage for the pristine and aged devices.

3.3. Interlayer Effects

To enhance hole injection and stabilize the hole injection in the PLED devices, a hole-transporting interlayer is inserted between the PEDOT:PSS hole-injection layer and the LEP. The purpose of the HTL is three-fold. First, this HTL should facilitate efficient hole injection. An ideal HTL will have a HOMO energy between the HOMO energy of the LEP and the PEDOT:PSS work function to facilitate hole injection. Second, it blocks the transport of electrons. Blocking of electrons requires the HTL with a small LUMO energy. Third, it acts as a buffer layer between the PEDOT:PSS layer and the LEP layer and eliminates the direct injection of electrons from the LEP layer to the PEDOT:PSS layer. As the device is solution processed, the HTL needs to be crosslinked and resistant to solvent processes. This crosslinkable HTL (XL-HTL)[69] enables spin coating of the LEP layer with good film-thickness control and prevents intermixing between the HTL and the LEP during the spin-coating process. **Figure 9** shows the current–voltage characteristics of the devices with and without the crosslinkable interlayer. Here, the thickness of the XL-HTL is 30 nm. From the figure, enhancement in hole injection that is due to the XL-HTL is quite apparent. The current density of the device with the XL-HTL is at least five times higher than that of the device with just a PEDOT:PSS injection layer. We have also observed similar enhancement in current density in dual-carrier devices with an XL-HTL. **Figure 10** shows the current efficiency as a

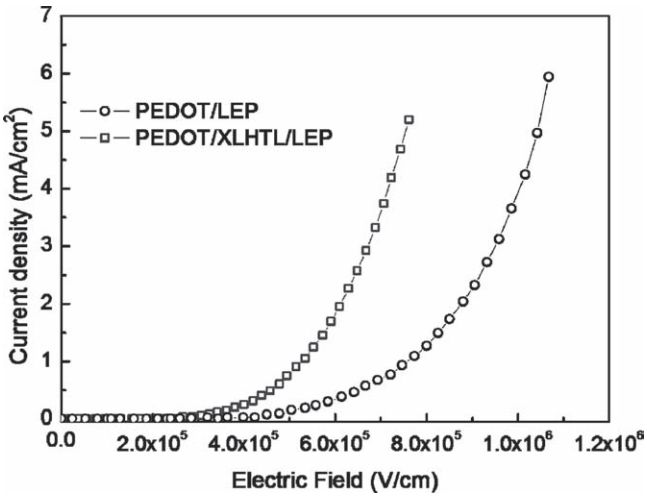

Figure 9. Current density versus electric field for devices with and without interlayer.

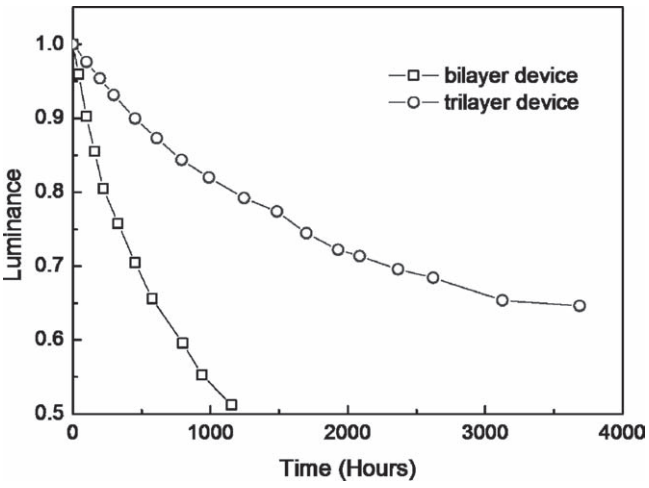

Figure 11. Device operating lifetime for devices with and without interlayer. Reproduced with permission.[69] Copyright 2007, American Institute of Physics.

function of electric field for PLED devices with and without the XL-HTL. The turn-on electric fields for both devices are about 2×10^5 V cm^{-1}. For the PEDOT device without the XL-HTL, the current efficiency does not reach its maximum until the electric field reaches about 4×10^5 V cm^{-1}. On the contrary, the current efficiency of the XL-HTL device rises sharply with the electric field and it reaches a value of 9 cd A^{-1} at an electric field of 2.3×10^5 V cm^{-1}. This enhancement charge balance along with the electron blocking due to the XL-HTL leads to higher device efficiency. It should be noted that the use of XL-HTL enhances the device efficiency over a large operating condition. The optimized, trilayer, green device shows a peak efficiency of 19 cd A^{-1}, which is almost twice the efficiency of the corresponding bilayer device. It should be noted that a similar effect on the PLED lifetime has been reported in devices with different HTLs. Kim et al.,[5] reported that using poly(2,7-(9,9-di-*n*-octylfluorene)-*alt*-(1,4-phenylene-((4-*sec*-butylphenyl)imino)-1,4-phenylene)) (TFB) as an interlayer on top of PEDOT:PSS resulted in a significant enhancement in efficiency. The authors concluded that the thin TFB interlayer acts as a buffer layer reducing exciton quenching leading to efficiency enhancement. It should also be noted that not all HTL enhances the device efficiency. For example, Lee et al.,[44] used a thermally treated poly(vinylcarbazole) (PVK) layer as an interlayer in PLEDs, and they observed that the device efficiency actually decreased due to the decreased hole mobility in the thermally treated interlayer.

In addition to the efficiency enhancement, the operating lifetime is also enhanced significantly because of the interlayer. **Figure 11** shows the lifetimes of both the PEDOT:PSS and the XL-HTL devices operated under multiplex conditions (multiplex ratio of 64). Here, the initial luminances of the PEDOT and the interlayer devices are 250 cd m^{-2} and 300 cd m^{-2}, respectively. As shown in **Figure 12**, the XL-HTL device shows a 7× enhancement in lifetime compared to the device without the XL-HTL. Because of the presence of the XL-HTL, the injection

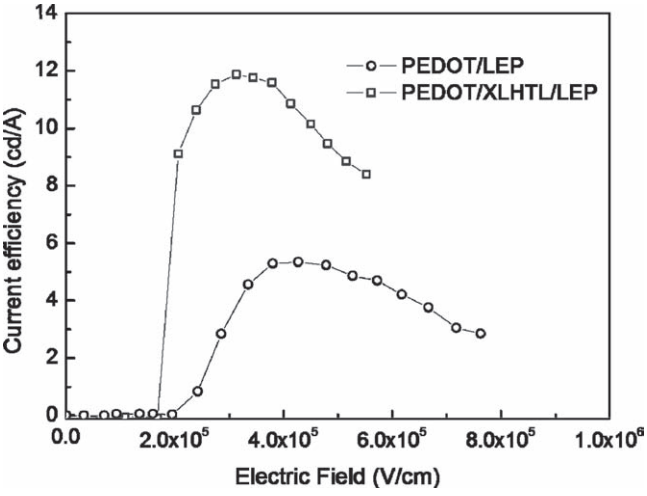

Figure 10. Current efficiency versus electric field for devices with and without interlayer.

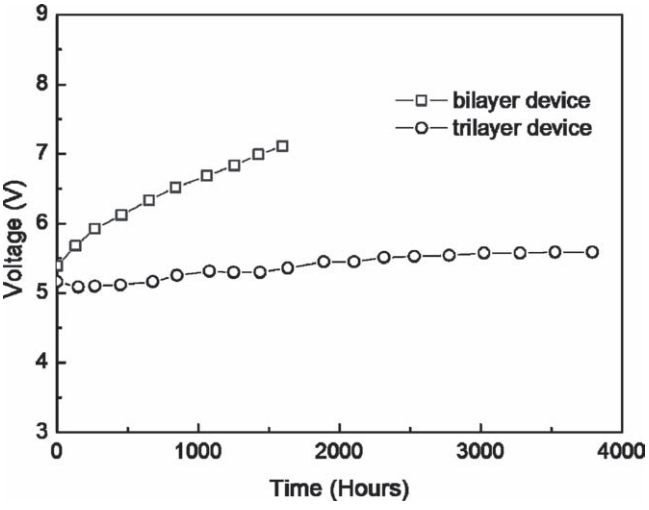

Figure 12. Operating voltage for devices with and without interlayer.

of electrons from the LEP layer into the PEDOT:PSS layer is blocked, and degradation to the PEDOT:PSS layer that is due to electrons is minimized, resulting in a better device stability. The enhanced luminance stability is also reflected from the voltage stability. Figure 7 shows the operating voltage as a function of time for devices with and without the XL-HTL. The device with the interlayer shows a very stable operating voltage over a period of several thousand hours, where the operation of the bilayer device shows a voltage rise of about 2 V during the first 1500 h.

4. Outlook

In this Progress Report, we have limited our discussions on degradation to fluorescent OLEDs. Degradation is a complex problem, and it took almost 20 years to understand some of the issues and to develop devices with sufficient stability for commercial product applications. On the other hand, while phosphorescent OLEDs are more efficient, their degradation mechanisms may be more complex because of the unique chemistries associated with organometallic molecules present as emitting dopants. We believe that some of the methodologies presented here will be useful to analyze the degradation processes in phosphorescent OLEDs as well as other organic-based optoelectronic devices.

Acknowledgements

F.S. acknowledges the experimental work performed by Dr. Dmitry Poplavskyy and Dr. Wencheng Su at OSRAM Opto Semiconductors. D.K. gratefully acknowledges the insightful discussions and experimental assistance of Dr. D. Giesen, Dr. V. V. Jarikov, Dr. J. R. Vargas, Dr. R. H. Young, M. Wojcik-Cross, R. L. Winter, D. A. Prosperi, and D. Comfort.

Received: August 3, 2009
Revised: September 25, 2009
Published online: May 20, 2010

[1] M. Pope, P. Magnante, H. P. Kallmann, *J. Chem. Phys.* **1963**, *38*, 2042.
[2] C. W. Tang, S. A. Vanslyke, *Appl. Phys. Lett.* **1987**, *51*, 913.
[3] C. Adachi, S. Tokito, T. Tsutsui, S. Saito, *Jpn. J. Appl. Phys., Part 2* **1988**, *27*, L269.
[4] T. Tsutsui, C. Adachi, S. Saito, *Acta Polytech. Scand., Appl. Phys. Ser.* **1990**, 145.
[5] J. S. Kim, R. H. Friend, I. Grizzi, J. H. Burroughes, *Appl. Phys. Lett.* **2005**, *87*, 023506.
[6] Y. Hamada, T. Sano, M. Fujita, T. Fujii, Y. Nishio, K. Shibata, *Jpn. J. Appl. Phys., Part 2* **1993**, *32*, L511.
[7] F. So, J. Kido, P. Burrows, *MRS Bull.* **2008**, *33*, 663.
[8] M. Uchida, Y. Ohmori, C. Morishima, K. Yoshino, *Synth. Met.* **1993**, *57*, 4168.
[9] D. D. C. Bradley, *Polym. Int.* **1991**, *26*, 3.
[10] D. Braun, A. J. Heeger, H. Kroemer, *J. Electron. Mater.* **1991**, *20*, 945.
[11] D. Braun, D. Moses, C. Zhang, A. J. Heeger, *Appl. Phys. Lett.* **1992**, *61*, 3092.
[12] N. C. Greenham, S. C. Moratti, D. D. C. Bradley, R. H. Friend, A. B. Holmes, *Nature* **1993**, *365*, 628.
[13] A. B. Holmes, D. D. C. Bradley, A. R. Brown, P. L. Burn, J. H. Burroughes, R. H. Friend, N. C. Greenham, R. W. Gymer, D. A. Halliday, R. W. Jackson, A. Kraft, J. H. F. Martens, K. Pichler, I. D. W. Samuel, *Synth. Met.* **1993**, *57*, 4031.
[14] S. Karg, W. Riess, V. Dyakonov, M. Schwoerer, *Synth. Met.* **1993**, *54*, 427.
[15] W. Bijnens, J. Manca, T. D. Wu, M. DOlieslaeger, D. Vanderzande, J. Gelan, W. DeCeuninck, L. DeSchepper, L. M. Stals, *Synth. Met.* **1996**, *83*, 261.
[16] Y. F. Liew, H. Aziz, N. X. Hu, H. S. O. Chan, G. Xu, Z. Popovic, *Appl. Phys. Lett.* **2000**, *77*, 2650.
[17] S. F. Lim, L. Ke, W. Wang, S. J. Chua, *Appl. Phys. Lett.* **2001**, *78*, 2116.
[18] Y. Sato, H. Kanai, *Mol. Cryst. Liq. Cryst. Sci. Tech., Mol. Cryst. Liq. Cryst.* **1994**, *252*, 435.
[19] S. Kim, C. Hsu, C. Zhang, H. Skulason, F. Uckert, D. LeCoulux, Y. Cao, I. Parker, *J. Soc. Inf. Disp.* **2004**, *5*, 14.
[20] *Current Injection in Solids*, (Eds: M. A. Lampert, P. Mark), Academic Press, New York **1970**.
[21] D. Poplavskyy, F. So, *J. of Appl. Phys.* **2006**, *99*.
[22] D. Poplavskyy, W. C. Su, F. So, *J. of Appl. Phys.* **2005**, *98*, 014501.
[23] S. A. Carter, M. Angelopoulos, S. Karg, P. J. Brock, J. C. Scott, *Appl. Phys. Lett.* **1997**, *70*, 2067.
[24] J. C. Scott, S. A. Carter, S. Karg, M. Angelopoulos, *Synth. Met.* **1997**, *85*, 1197.
[25] D. Y. Kondakov, J. R. Sandifer, C. W. Tang, R. H. Young, *J. of Appl. Phys.* **2003**, *93*, 1108.
[26] M. Ariu, D. G. Lidzey, M. Sims, A. J. Cadby, P. A. Lane, D. D. C. Bradley, *J. Phys.: Condens. Matter* **2002**, *14*, 9975.
[27] A. W. Grice, D. D. C. Bradley, M. T. Bernius, M. Inbasekaran, W. W. Wu, E. P. Woo, *Appl. Phys. Lett.* **1998**, *73*, 629.
[28] N. A. Iyengar, B. Harrison, R. S. Duran, K. S. Schanze, J. R. Reynolds, *Macromolecules* **2003**, *36*, 8978.
[29] Q. Peng, Z. Y. Lu, Y. Huang, M. G. Xie, S. H. Han, J. B. Peng, Y. Cao, *Macromolecules* **2004**, *37*, 260.
[30] H. Murata, C. D. Merritt, H. Inada, Y. Shirota, Z. H. Kafafi, *Appl. Phys. Lett.* **1999**, *75*, 3252.
[31] Y. Shirota, K. Okumoto, H. Inada, *Synth. Met.* **2000**, *111*, 387.
[32] K. Okumoto, T. Ohara, T. Noda, Y. Shirota, *Synth. Met.* **2001**, *121*, 1655.
[33] C. Adachi, K. Nagai, N. Tamoto, *Appl. Phys. Lett.* **1995**, *66*, 2679.
[34] G. C. M. Silvestre, M. T. Johnson, A. Giraldo, J. M. Shannon, *Appl. Phys. Lett.* **2001**, *78*, 1619.
[35] H. Aziz, Z. D. Popovic, N. X. Hu, A. M. Hor, G. Xu, *Science* **1999**, *283*, 1900.
[36] Y. Hamada, T. Sano, K. Shibata, K. kuroki, *Jpn. J. Appl. Phys.* **1995**, *34*, L824.
[37] A. W. D. Van Der Gon, J. Birgerson, M. Fahlman, W. R. Salaneck, *Org. Electron.* **2002**, *3*, 111.
[38] V. E. Choong, S. Shi, J. Curless, F. So, *Appl. Phya. Lett.* **2000**, *76*, 958.
[39] V. E. Choong, J. Shen, J. Curless, S. Shi, J. Yang, F. So, *J. Phys. D* **2000**, *33*, 760.
[40] V. E. Choong, S. Shi, J. Curless, C. L. Shieh, H. C. Lee, F. So, J. Shen, J. Yang, *Appl. Phys. Lett.* **1999**, *75*, 172.
[41] Z. D. Popovic, H. Aziz, C. P. Tripp, N. X. Hu, A. M. Hor, G. Xu, *Proc. SPIE* **1999**, *68*, 3476.
[42] A. B. Chwang, R. C. Kwong, J. J. Brown, *Appl. Phys. Lett.* **2002**, *80*, 725.
[43] C. H. Hsiao, Y. H. Chen, T. C. Lin, C. C. Hsiao, J. H. Lee, *Appl. Phys. Lett.* **2006**, *89*.
[44] T. W. Lee, M. G. Kim, S. Y. Kim, S. H. Park, O. Kwon, T. Noh, T. S. Oh, *Appl. Phys. Lett.* **2006**, *89*, 123505.

[45] J. Curless, S. Rogers, M. Kim, M. Lent, S. Shi, V. E. Choong, C. Briscoe, F. So, *Synth. Met.* **1999**, *107*, 53.
[46] M. P. de Jong, L. J. van IJzendoorn, M. J. A. de Voigt, *Appl. Phys. Lett.* **2000**, *77*, 2255.
[47] T. M. Brown, J. S. Kim, R. H. Friend, F. Cacialli, R. Daik, W. J. Feast, *Synth. Met.* **2000**, *111*, 285.
[48] R. H. Young, J. R. Lenhard, D. Kondakov, T. K. Hatwar, *Proc. Soc. Inf. Disp.* **2008**, *39*, 705.
[49] M. Yahiro, D. C. Zou, T. Tsutsui, *Synth. Met.* **2000**, *111*, 245.
[50] D. Y. Kondakov, *J. Soc. Inf. Disp.* **2009**, *17*, 137.
[51] H. J. Ding, K. Park, Y. L. Gao, D. Y. Kim, F. So, *Chem. Phys. Lett.* **2009**, *473*, 92.
[52] F. Rohlfing, T. Yamada, T. Tsutsui, *J. Appl. Phys.* **1999**, *86*, 4978.
[53] D. Y. Kondakov, T. D. Pawlik, W. F. Nichols, W. C. Lenhart, *J. Soc. Inf. Disp.* **2008**, *16*, 37.
[54] D. Y. Kondakov, W. C. Lenhart, W. F. Nichols, *J. Appl. Phys.* **2007**, *101*, 024512.
[55] D. Y. Kondakov, *J. Appl. Phys.* **2007**, *102*, 084520.
[56] R. Meerheim, S. Scholz, S. Olthof, G. Schwartz, S. Reineke, K. Walzer, K. Leo, *J. Appl. Phys.* **2008**, *104*.
[57] N. J. Turro, *Modern Molecular Photochemistry*, University Science Books, Sausolitos CA, USA **1991**, p. 183.
[58] S. Janietz, D. D. C. Bradley, M. Grell, C. Giebeler, M. Inbasekaran, E. P. Woo, *Appl. Phys. Lett.* **1998**, *73*, 2453.
[59] B. Liu, M. A. McCarthy, Y. Yoon, D. Y. Kim, Z. C. Wu, F. So, P. H. Holloway, J. R. Reynolds, J. Guo, A. G. Rinzler, *Adv. Mater.* **2008**, *20*, 3605.
[60] M. M. de Kok, M. Buechel, S. I. E. Vulto, P. van de Weijer, E. A. Meulenkamp, S. H. P. M. de Winter, A. J. G. Mank, H. J. M. Vorstenbosch, C. H. L. Weijtens, V. van Elsbergen, *Phys. Status Solidi A* **2004**, *201*, 1342.
[61] J. S. Kim, P. K. H. Ho, C. E. Murphy, N. Baynes, R. H. Friend, *Adv. Mater.* **2002**, *14*, 206.
[62] K. R. Choudhury, J. W. Lee, N. Chopra, A. Gupta, X. Z. Jiang, F. Amy, F. So, *Adv. Funct. Mater.* **2009**, *19*, 491.
[63] N. Chopra, J. Lee, Y. Zheng, S. H. Eom, J. E. Xue, F. So, *ACS Appl. Mater. Interfaces* **2009**, *1*, 1169.
[64] N. Chopra, J. Lee, Y. Zheng, S. H. Eom, J. G. Xue, F. So, *Appl. Phys. Lett.* **2008**, *93*.
[65] T. M. Brown, J. S. Kim, R. H. Friend, F. Cacialli, R. Daik, W. J. Feast, *Appl. Phys. Lett.* **1999**, *75*, 1679.
[66] M. C. Suh, H. K. Chung, S. Y. Kim, J. H. Kwon, B. D. Chin, *Chem. Phys. Lett.* **2005**, *413*, 205.
[67] C. Giebeler, S. A. Whitelegg, D. G. Lidzey, P. A. Lane, D. D. C. Bradley, *Appl. Phys. Lett.* **1999**, *75*, 2144.
[68] R. U. A. Khan, D. D. C. Bradley, M. A. Webster, J. L. Auld, A. B. Walker, *Appl. Phys. Lett.* **2004**, *84*, 921.
[69] F. So, B. Krummacher, M. K. Mathai, D. Poplavskyy, S. A. Choulis, V. E. Choong, *J. Appl. Phys.* **2007**, *102*, 091101.